Fatigue and cracking behaviour of austenitic CrNiMo and CrMnN steels in chloride containing environment at elevated temperature

Clemens Vichytil[1], Gregor Mori[1], Reinhard Pippan[2], Michael Panzenböck[3] and Rainer Fluch[4]

[1] Christian Doppler Laboratory of Localized Corrosion, Department of General, Analytical and Applied Chemistry, Montanuniversität Leoben, Franz-Josef Straße 18, A-8700 Leoben, Austria

[2] Erich Schmid Institut of Materials Science, Austrian Academy of Science, Jahnstraße 12, A-8700 Leoben, Austria

[3] Department of Physical Metallurgy and Materials Testing, Montanuniversität Leoben, Franz-Josef Straße 18, A-8700 Leoben, Austria

[4] Bohler Special Steels GmbH & Co KG, Research and Development Special Materials, Mariazeller Straße 25, A-8605 Kapfenberg, Austria

[1]clemens.vichytil@unileoben.ac.at

Keywords: corrosion fatigue, austenitic stainless steels, crack growth rate.

Purpose: Austenitic stainless steels are often used for applications under combined mechanical and chemical loading. Corrosion fatigue behaviour, electrochemistry and crack growth rate curves of different austenites have been investigated to determine failure processes and damage mechanisms.
Approach: CrMnN austenites possess better mechanical properties and have been developed to replace CrNiMo stabilized ones in certain applications. Different steels of both types have been studied in this research. S/N curves and crack propagation rate curves have been recorded in inert glycerine as a reference, and in 43 wt-% $CaCl_2$ solution. As testing temperature 120°C was used. Electrochemical behaviour and repassivation potential of the materials has also been tested.
Findings: CrNiMo steels possess excellent corrosion properties, even in very aggressive environments as 43 wt-% $CaCl_2$ solution at 120°C. These steels do not show a distinctive susceptibility to stress corrosion cracking in this medium, not even if mechanical properties are increased by cold working. Crack propagation of CrNiMo austenites is even lower in corrosive environment compared to inert glycerine and fatigue strength is moderately reduced.
CrMnN grades possess excellent mechanical properties, but they are very susceptible to stress corrosion cracking and are less corrosion resistant compared to CrNiMo steels. Fatigue strength and threshold for long crack growth are significantly reduced in this severe environment, and crack propagation is extremely pronounced in the near threshold region.
Results are compared and possible explanations of the different behaviours are critically discussed.

Introduction

For applications in high chloride containing environments austenitic stainless steels are commonly used. The two major families of austenitic stainless steels are conventional CrNi steels and CrMnN steels. CrNi steels have been investigated in various hot chloride solutions [1,2,3,4,5,6]. Although CrMnN steels have a high potential in replacing CrNi steels in some applications, hardly any data on

corrosion fatigue (CF) or crack growth rates of these steels can be found. CrMnN steels stand out through their high strength and pronounced elongation at fracture. CrNi steels on the other hand have distinctive corrosion resistance and are more resistant to chloride containing aqueous solution compared to CrMnN steels.

It is well documented in literature that several failure mechanisms can be responsible for crack formation and propagation in austenitic stainless steels. Investigations that contributed to a more fundamental understanding of CF mechanisms were published by Magnin [3,4,7,8,9]. These mechanisms strongly depend on applied potential. According to Magnin there are five different damage mechanisms for passive metals exposed to corrosion fatigue loads between the cathodic and transpassive potential ranges of the polarization curve.

From cyclic polarization curves information about the electrochemistry of passivizing steels may be gained, but a clear definition of pitting potential or repassivation potential is hardly possible as the electrolyte is continuously changing in pits. Stainless steels are in general only corrosion resistant as long as their passive film is stable or undamaged. If however the passive film is damaged by e.g. slip steps, the repassivation behaviour of this material in a specific environment becomes important. It has already been shown by H.S. Kwon et al. and K.A. Yeom et al. [10,11] that stress corrosion cracking susceptibility may be predicted by repassivation kinetics. In recent years mostly CrNiMo austenitic stainless steels have been investigated with different methods [12,13,14,15,16,17,18,19,20,21,22]. All these works, especially by H.S. Kwon and T. Burstein [10,16,17,18] lead to a general understanding of repassivation mechanisms. However, hardly any experimental data could be found regarding repassivation in high Cl^- (>300000 ppm) containing environments at elevated temperatures (>100°C). Furthermore repassivation without applying a potential on the tested sample has not been investigated in detail. This is of great importance, as neither structures nor applications of austenitic stainless steels are cathodically protected. Moreover hardly any data of the repassivation of CrMnN steels could be found.

Crack growth rates of austenitic stainless steels have been measured with different methods in mild corrosive environments [23,24,25,26,27,28,29]. No publications of crack growth measurements of CrMnN and CrNi steels under above mentioned conditions have been found. The influence of the aqueous solution on the crack growth rate was compared to measurements in air as an inert medium. An increase of the crack growth rate by aqueous solution was found in some cases [24,27,28,29] while no difference could be observed in others [25,26,28]. Speidel [25] has found a great difference in crack growth rate between air and vacuum. He states that air itself is an aggressive environment and does enhance crack growth rate significantly. Endo et al. [27] observed that increasing Cl^- ion concentration will enhance local dissolution of the metal. Initiation of cracks often occurs through a localized attack of the environment such as pitting corrosion [26].

CF and stress corrosion cracking (SCC) are two corrosion phenomena which show similar mechanisms. Pure CF hardly ever takes place and an overlap with SCC, especially during crack initiation and propagation, is likely to be observed. A clear distinction between CF and SCC is, as yet, not possible by simple investigation of the fracture surfaces, because both cracking modes result in similar characteristics on the fracture surfaces. Transgranular cleavage-like structures [30], facetted cleavage, crack arresting marks and factory roof structures [8,31] can be observed on fracture surfaces of samples which failed under cyclic or static loading in corrosive environment.

The aim of the present research is to show and compare CF and crack propagation behaviour of different CrNiMoN and CrMnN stabilized steels. Moreover a better understanding of failure mechanisms in hot, high chloride containing environments of both steel types shall be achieved. An empiric model can be derived from the collected results, which allows a prediction of CF and SCC behaviour of different austenitic stainless steels in specific environments.

Materials and Sample Preparation

Four different austenitic stainless steels, two CrNiMo and two CrMnN stabilized, were investigated in solution annealed condition. Chemical compositions and PREN 3[32] (pitting resistance equivalent number) are listed in Table 1, PREN was calculated according to Eq. 1. Mechanical properties of all materials tested in glycerine at 120°C are listed in Table 2.

PREN = wt-%Cr + 3.3 wt-% Mo + 20 wt-% N (1)

Table 1: Chemical composition and PREN of investigated materials

Material	C	Cr	Mn	Ni	Mo	N	PREN
CrNiMo28-30-3	0.02	26-29	2-3.5	28-31	2-4.5	0.2-0.35	~42
CrNiMo18-14-3	≤ 0.03	17.5	1.7	14.5	2.7	0.07	~29
CrMnN18-21-.6	≤ 0.06	18.2	21.2	1.7	0.5	0.6	~33
CrMnN21-24-1	≤ 0.06	21.3	23.4	1.5	0.2	0.9	~40

Table 2: Mechanical properties of investigated materials at 120°C

Material	$R_{p0,2}$ [MPa]	R_m [MPa]	Elongation at Fracture A_5 [%]
CrNiMo28-30-3	300	690	62
CrNiMo18-14-3	240	500	54
CrMnN18-21-.6	420	780	59
CrMnN21-24-1	455	860	62

CF samples were longitudinally turned according to ASTM E466. The gauge diameter of the specimens was 8 mm with a parallel length of 10 mm. Samples for electrochemical measurements have been machined from the same rods. These samples were approximately 20 mm in diameter and 5 mm in thickness. The dimensions of the repassivation specimen were 5 mm in diameter and 17 mm in length. All samples were electro polished using a H_3PO_4-H_2SO_4 based electrolyte and approximately 100 µm and any non-metallic inlcusions were removed from the surface. Compact tension (CT) specimens for crack growth rate measurements were machined according to ASTM E647. Specimens were machined out of the rod material that crack growth direction was in radial direction [32]. CT-specimens were mechanically polished and precracked under cyclic compression to gain an "open" crack tip due to residual tension stresses at the crack tip 31[33,34]. For precracking a cyclic stress intensity factor (ΔK) of 20 MPa√m at a stress ratio (R-value) of 20 was used. This resulted in a precrack of approximately 100 µm.

CF tests were carried out with calibrated servo-hydraulic testing machines with a 32 kN and a 50 kN load cell respectively. Tests were performed in double walled glass cells, heated with a thermostat and temperature controlled with a Pt-100 temperature sensor. The amount of testing solution was 500 ml. S/N curves were recorded according to DIN 50100. The experiments were carried out under load control and at each stress level 3 specimens were tested. The fatigue limit was defined as the stress level where all 3 samples endured at least $1.2 * 10^7$ cycles (equivalent to 7 days testing time) and it was determined with an accuracy of 10 MPa. A more detailed description of the experimental setup can be found in [32]. The direct current potential drop method (DCPD) was used to measure crack propagation. The same calibrated servo-hydraulic testing machines but with a 5 kN load cell were used. The initial ΔK was 2 MPa√m and increased by steps of 0.5 MPa√m every $1.7 * 10^6$

cycles (24 h) if no crack propagation occurred. A more detailed description of the experimental setup and testing procedure can be found in [35].
For all mechanical experiments 43wt-% $CaCl_2$ solution was used as corrosive environment and inert glycerine as reference medium. Testing temperature was 120°C and a frequency of 20 Hz has been applied, as this frequency resembles possible application loading frequency. An R-value of 0.05 was chosen to apply pure tensile stresses.
Cyclic polarization curves and repassivation kinetics were measured in 43wt-% $CaCl_2$ solution at 120°C, and 25°C as well as in 3wt-% $CaCl_2$ solution at 70°C and 25°C. A scan rate of 200 mV/h, a platinum sheet as counter electrode and an Ag/AgCl reference electrode were used. Before the potentiodynamic scan the open circuit potential (OCP) has been measured for 1 hour.
All measurements were performed without impressing a potential on the sample and as counter electrode the same material as the working electrode (repassivation specimen) was used. Hence all experiments were performed under open circuit potential. Before each measurement the equilibrium potential of counter and working electrode was measured for approximately 60 minutes versus the Ag/AgCl reference electrode. After potential measurements working and counter electrode were short-circuited. Short circuiting lead to a short current peak, but within several seconds no significant current was detectable (I <50 [nA]). Due to this short current peak a minimum period of 90 seconds was awaited, before activation of the working electrode by scratching was performed. The current, if repassivation occurred, was measured until it declined to values < 50 [nA]. The sample rate was always .1 s.
Fracture surfaces of selected samples from CF and fatigue crack growth tests were investigated by scanning electron microscope (SEM).

Results

Corrosion Fatigue Testing. All materials show a decrease in fatigue strength in 43 wt-% $CaCl_2$ at 120°C. Table 3 gives an overview of the fatigue strength and its decrease, which was calculated by Eq. 2.

$$\text{Decrease of Fatigue Strength [\%]} = \left[1 - \left(\frac{\text{Fatigue Strength in 43wt}-\%\ CaCl_2}{\text{Fatigue Strength in Glycerine}}\right)\right] \times 100 \quad (2)$$

Specimen with a yield to fatigue strength ratio of 0.5 were chosen for fracture surface analysis and comparison. This was done as all four materials possess different yield and tensile strengths. In glycerine all materials show a typical transgranular fatigue cracking, documentation may be found elsewhere [32].
In 43 wt-% $CaCl_2$ solution circumferential and fracture surfaces exhibit different details and cracking modes. At all materials slip step dissolution occurs, but it is pronounced at the CrMnN alloys (Fig. 1a). Both CrMnN alloys show the same fracture surface characteristics, hence only SEM pictures of the CrMnN18-21-.6 are shown. The CrNiMo materials show also slight dissolution of slip steps (Figs. 1b and c) and in the case of the lower alloyed material some massive oxide layers around the initiation point of fracture (Fig. 1b). In the vicinity of the initiation point of fracture pure transgranular cleavage like fracture surface is visible at the CrMnN materials (Fig. 1d), but transgranular fatigue fracture with some significant amounts of oxide layers or corrosion debris at the CrNiMo alloys (Figs. 1e and f). With increasing crack length the CrMnN austenites exhibit no fatigue typical striations, but mainly cleavage cracking with factory roof structures (Fig. 1g). The lower alloyed CrNiMo shows some intergranular cracking with slightly dissolved grain boundaries (Fig. 1h), whereas the higher alloyed CrNiMo exhibits a pure transgranular fatigue crack with very fine striations (Fig. 1i). On the overload fracture, both, the CrMnN and the lower alloyed CrNiMo austenite show some branched crack network (Figs. 1j and k). The higher alloyed CrNiMo just shows a ductile rupture (Fig. 1l).

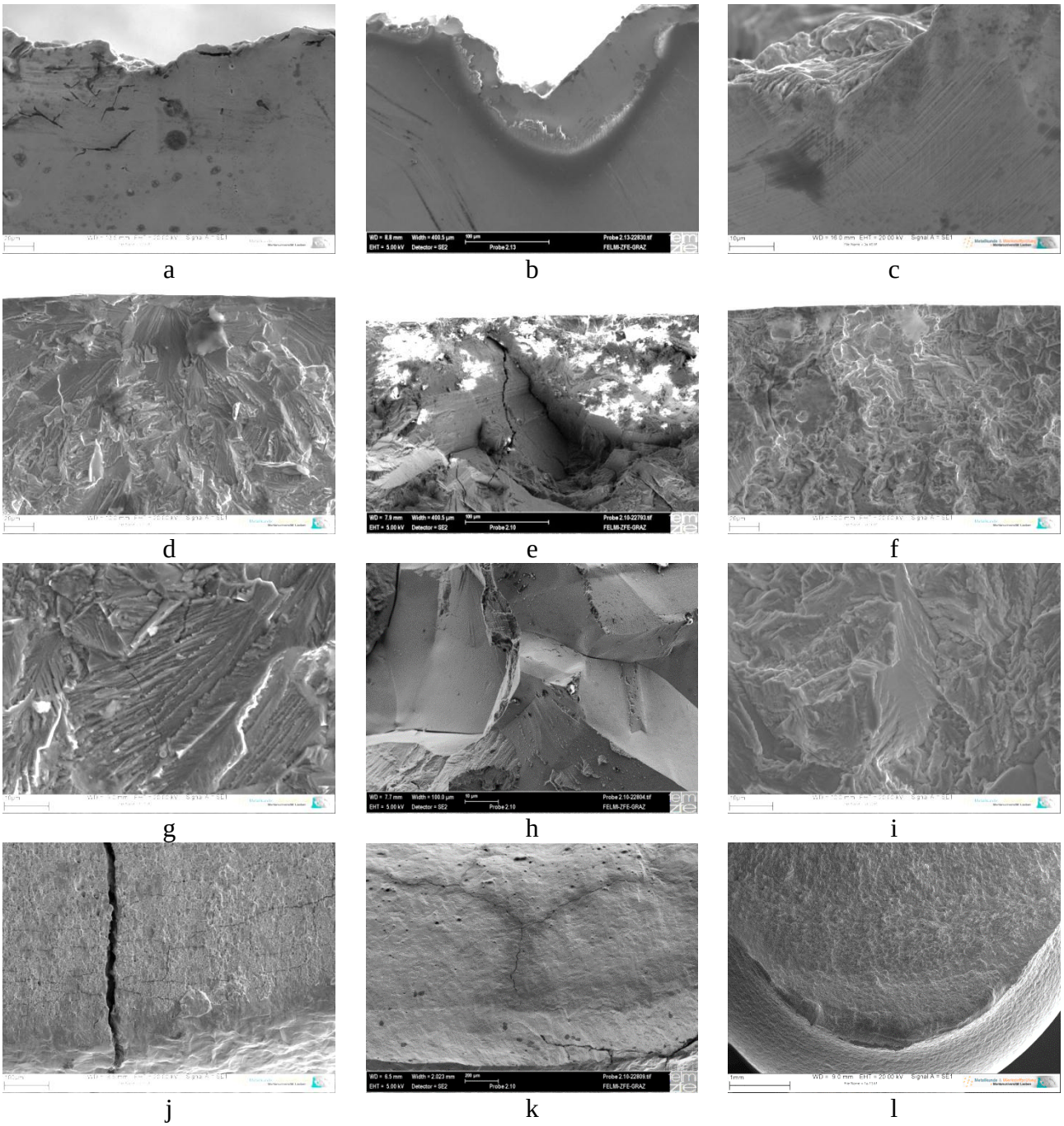

Figure 1: Fatigue specimen tested in 43 wt-% $CaCl_2$ solution at 120°C, f=20 Hz, R=0.05
CrMnN18-21-.6, $1.3*10^5$ cycles to failure at 400 MPa, dissolved slip steps on sircumference of specimen (a), facetted cleavage at initiation point of fracture (d), detail of fracutre surface with factory roof structure (g) and branched crack network on overload fracture (j)
CrNiMo18-14-3, $3.5*10^6$ cycles to failure at 240 MPa, secondary corrosion products on circumference of specimen (b), oxide layers around crack initiation (e), intergranular fracture with slightly dissolved grain boundaries (h) and branched cracks on overload fracture surface (k)
CrNiMo28-30-3, $8.2*10^6$ cycles to failure at 320 MPa, slightly dissolved slip steps on circumference of specimen (c), initiation point of fracture with oxide layers (f), detail of fracture surface with very fine striations (i), overload fracture surface with pure ductile rupture (l)

Table 3: Fatigue limits of investigated materials

Material	Medium	Fatigue limit [MPa]	Fatigue limit decrease [%]
CrNiMo28-30-3	Glycerine	340±10	20
	43wt-% $CaCl_2$	270±10	
CrNiMo18-14-3	Glycerine	260±10	15
	43wt-% $CaCl_2$	220±10	
CrMnN18-21-.6	Glycerine	380±10	24
	43wt-% $CaCl_2$	290±10	
CrMnN21-24-1	Glycerine	400±10	28
	43wt-% $CaCl_2$	290±10	

Crack Propagation testing. Crack growth rate curves of the materials CrNiMo28-30-3, CrNiMo18-14-3 and CrMnN18-21-.6 are shown in Fig. 2. In inert glycerine precritical crack growth occurred several times until the threshold for long crack growth was reached. For solution annealed condition the threshold is 12.5 MPa√m for the CrNiMo28-30-3 austenite and 9 MPa√m for the CrMnN18-21-.6 material. The lower alloyed CrNiMo material shows a comparable behaviour to the CrNiMo28-30-3 in inert glycerine. In 43 wt-% $CaCl_2$ solution, the threshold is significantly decreased to values of 2.5 to 3.5 for all materials. More data of these materials is available elsewhere [36,37]. Precritical crack growth and crack arrest was only observed at the higher alloyed CrNiMo and the CrMnN 18-21-.6 material. At both steels cracks propagated continuously after an increase of .5 MPa√m. Surprisingly in corrosive environment cracks in the CrNiMo materials exhibit a crack propagation rate of about one order of magnitude smaller compared to inert glycerine. In both materials cracks propagate very slowly. SEM investigations of the fracture surfaces exhibit transgranular fatigue fracture, with significant amounts of oxide layers and very fine striations at both CrNiMo materials, whereas the CrMnN steel shows facetted cleavage, corrosion debris and pitting corrosion but no striations at all. CT specimen of the CrMnN material failed after a couple of hours, whereas the CrNiMo experiments lasted for at least 20 days in corrosive environment. In general fracture surfaces details are in all cases comparable to fracture surfaces of fatigue samples.

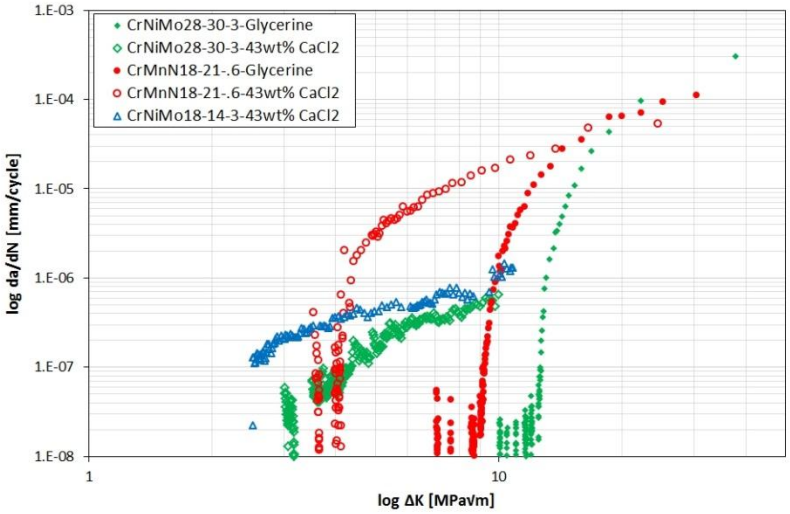

Figure 2: Crack propagation curves of CrNiMo28-30-3, CrNiMo18-14-3 and CrMnN18-21-.6 in glycerine and 43 wt-% $CaCl_2$ solution at 120°C, f=20 Hz, R=0.05

Electrochemistry. To characterize the electrochemical properties of the materials under testing conditions, cyclic polarization curves have been recorded in 43 wt-% CaCl2 at 120°C. To gain information about application limits and influence of Cl^- content and temperature, cyclic polarization curves were also recorded at various temperatures ranging from ambient to 120° in 43 wt-% $CaCl_2$ solution and from ambient to 70°C in 3 wt-% $CaCl_2$ solution. One representative curve of each material recorded in 43 wt-% $CaCl_2$ solution at 120°C can be seen in Fig. 3a. Both CrNiMo materials exhibit a wide passive range of about 140 mV, whereas the CrMnN materials do not show any passive range at these testing conditions. It is no surprise that the much higher alloyed CrNiMo28-30-3 material is nobler compared to the lower alloyed CrNiMo18-14-3 austenite. Inserted in Fig. 3a are two cyclic polarization specimens after testing, of which the left specimen is representative for the CrMnN material, showing a shallow and circular attack initiated at pits. The right specimen shows the corrosive attack on the CrNiMo materials. It starts by localized break down of the passive layer and is also shallow but more widespread compared to the CrMnN materials. Moreover the CrNiMo materials should be able to repassivate in 43 wt-% $CaCl_2$ solution, as the repassivation potentials are more noble than the open circuit potential. In Fig. 3b two cyclic polarization curves of the higher alloyed CrMnN21-24-1 in 3 wt-% $CaCl_2$ solution at ambient temperature and 70°C are shown. With increasing temperature, the passive range clearly declines. Nevertheless, a very wide passive range of approximately 1000 mV is present at ambient temperatures.

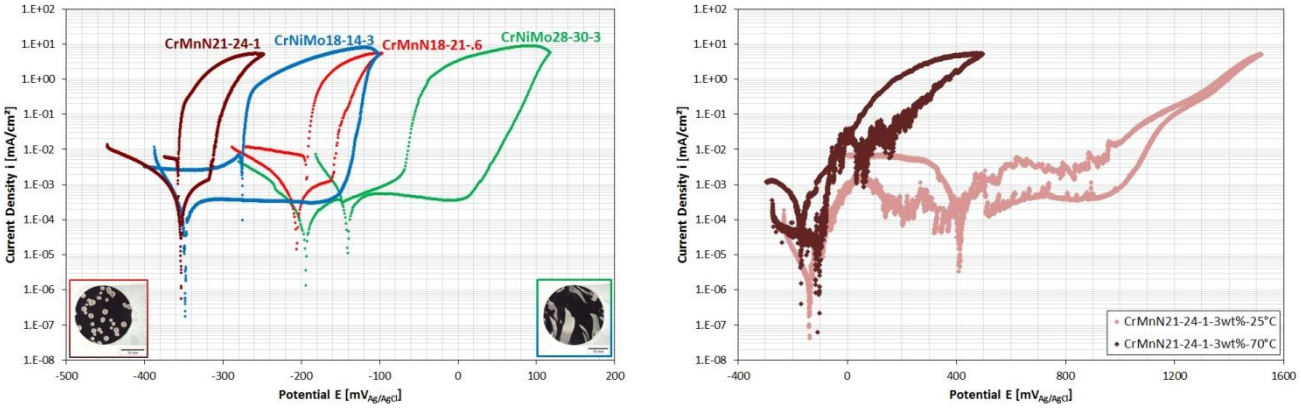

a b

Figure 3: Cyclic polarization curves of CrNiMo28-30-3, CrNiMo18-14-3, CrMnN18-21-.6 and CrMnN21-24-1 in 43 wt-% $CaCl_2$ solution at 120°C (a) and CrMnN18-21-.6 and CrMnN21-24-1 in 3 wt-% $CaCl_2$ solution at 25°C and 70°C (b), Pt counter electrode, Ag/AgCl reference electrode, 200 mV/h scan rate

Repassivation. Figs. 4a and b show repassivation curves of the materials CrNiMo28-30-3, CrNiMo14-18-3 and CrMnN21-24-1 in 43 wt-% $CaCl_2$ solution at 120°C and in 3 wt-% $CaCl_2$ solution at 70°C. Both CrNiMo materials repassivate nicely in very corrosive environment (Fig. 4a). The CrMnN on the other hand shows an inclination point, but no repassivation occurs. Under milder conditions, 3 wt-% $CaCl_2$ solution and 70°C, all materials show good repassivation properties at open corrosion potential. In some way this is surprising, as in the case of the CrMnN material no distinctive passive range was present under these conditions.

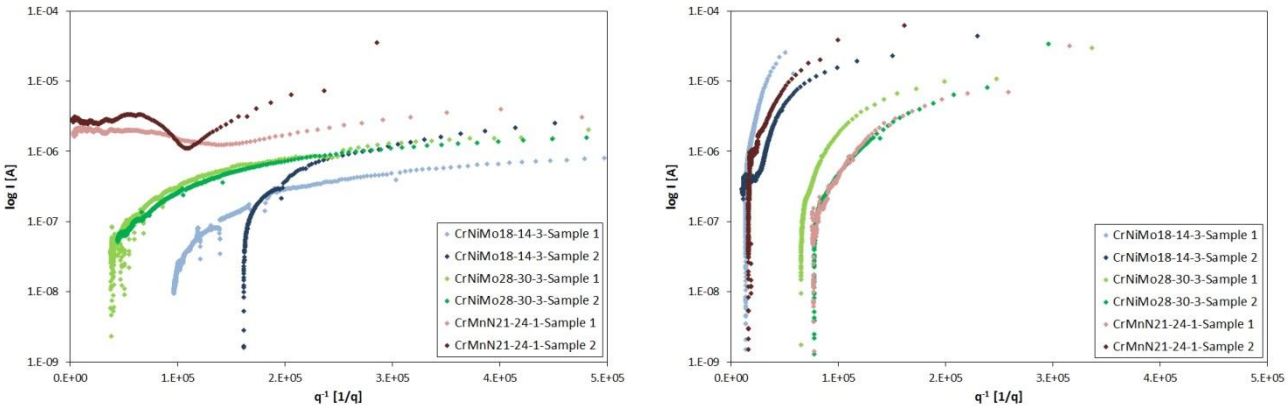

a b

Figure 4: Repassivation curves of CrNiMo28-30-3, CrNiMo14-18-3 and CrMnN21-24-1 in 43 wt-% $CaCl_2$ solution at 120°C (a) and in 3 wt-% $CaCl_2$ solution at 70°C

Discussion

In 43wt-% $CaCl_2$ solution fatigue strength is decreased in all materials. The slip step dissolution mechanisms seems to be responsible for the initiation of fatigue damage in corrosive environment in all investigated alloys. If the passive layer of chemically stable steels is damaged by evolving slip steps or extrusions and intrusions, bare steel is contacted with the surrounding environment and cannot repassivate immediately. Consequently a chemical reaction of the bare steel with the aqueous chloride solution takes place. Due to the chemical attack, cracks are initiated earlier compared to inert glycerine. In the case of the CrMnN steels a clear dissolution of the slip steps is visible, moreover pitting occurs on the circumferential surface, where cracks may also initiate. From the electrochemical measurements it is known that this steel does not possess a passive range and also does not repassivate in 43 wt-% $CaCl_2$ solution, once the passive layer is damaged. Moreover typical signs for SCC were found on the fracture surfaces, like facetted cleavage and factory roof structure. Hence it is clear, that this steel is strongly susceptible to stress corrosion cracking in 43 wt-% $CaCl_2$ solution. This is also fortified by the branched network of secondary cracks on the overload fracture surface. The lower alloyed CrNiMo18-14-3 has a pronounced passive range, and excellent repassivation properties. The excellent corrosion resistance of both CrNiMo steels has been shown by the cyclic polarization and the repassivation curves. Nevertheless significant amounts of oxides are found on the circumferential and fracture surface of the CrNiMo18-14-3. The oxide layers were all identified by EDX-Analysis and are all of a comparable chemical composition. These oxides are mainly secondary corrosion products which are deposited behind the crack tip. Also the higher alloyed CrNiMo28-30-3 shows some oxide layers on the fracture surface, but as this steel is much higher alloyed and consequently more nobel, which is mainly due to its high nickel content, less corrosion products are produced.

The 43 wt-% $CaCl_2$ solution also seems to be very selective, as the fracture surfaces of CrNiMo18-14-3 specimen show some intergranular cracking. This steel has very low carbon and no sensitization has occurred, hence intergranular corrosion can be ruled out. Moreover, no precipitations were found at any grain boundary, neither on the fracture surface nor on metallographic specimen. The testing solution contains a very high amount of Cl^- (> 300 000 ppm), but investigated CrNiMo alloys are moderately attacked by the solution in regard of its chloride content and temperature. Grain and twin boundaries as well as slip steps are usually at more ignoble potentials (higher activity) compared to the bulk material, hence corrosive attack preferably takes place at these more active sites. Intergranular cracking of CrNiMo18-14-3 samples can be explained by this selective attack. The higher alloyed and more noble CrNiMo28-30-3 just shows

transgranular fatigue cracking. At this stage no conclusion can be drawn to what extent the intergranular cracking influences the corrosion fatigue cracking mechanism. As branched secondary cracks were present on the overload fracture surface, it seems likely that this steel is also susceptible to SCC in 43 wt-% $CaCl_2$ solution, but not as pronounced as the CrMnN alloys. No obvious interference of SCC with CF could be observed during the investigations at the CrNiMo28-30-3 alloy. If crack propagation rate curves are taken into account, indicating a much slower crack growth in corrosive environment, SCC can be ruled out. Concluding it can be stated, that even in high chloride concentration solutions at elevated temperatures, SCC as dominant failure mechanism can be ruled out for the CrNiMo27-30-3 grade. The less alloyed CrNiMo grade however is susceptible to SCC in 43 wt-% $CaCl_2$ solution at 120°C [37], but crack propagation is still low and reduction in fatigue strength is just 15%. The amount of alloying elements Cr, Ni and Mo seems to play a major role towards the susceptibility to SCC of steels of the CrNiMo group in solutions with extreme high amounts of Cl^- (e.g.43 wt-% $CaCl_2$ solution) and temperatures >100°C. The formed oxide layers or corrosion debris are the main cause for the retarded crack propagation of the CrNiMo steels under severe corrosion conditions, like 43 wt-% $CaCl_2$ solution and 120°C. In glycerine, roughness and plasticity induced crack closure are the reasons for crack stopping after precritical crack growth. As hardly any chemical reaction takes place in inert glycerine, but in corrosive environments, oxide or corrosion debris induced crack closure significantly attributes to retarded crack propagation. It has yet not been clearly understood why crack propagation is below $1*10^{-7}$ mm/cycles close to the threshold value in the CrNiMo steels (Fig. 2). More experiments will be carried out to understand this surprising behaviour. In case of the CrMnN steel, severe corrosive attack was visible on the fracture surfaces. Pitting occurred and also secondary corrosion products were found, comparable to the ones of the CrNiMo steels. Oxide induced crack closure has an effect on crack propagation in this alloy as well, but as this steel is strongly susceptible to SCC in this specific environment, acceleration of cracks by SCC is predominant.

An interference of SCC and CF is possible as both corrosion phenomena show similar mechanisms. It is not unusual that SCC interferes with CF during crack initiation and propagation but evidence can be found on the fracture surfaces (e.g. cleavage-like structures, factory roof structures, branched SCC cracks etc., Figs 1d and g). If steels susceptible to SCC in a certain medium are exposed to cyclic loading in the same medium, a clear separation of SCC to CF is hardly possible. A definite interference of SCC and CF is present at the CrMnN alloys, as typical signs for SCC where found on fracture surfaces of all samples. Branched cracking during experiments under cyclic loading, as well as sudden and fast crack propagation at low stress intensity factors prove an SCC-CF overlap. Increasing amounts of Cr, Mn and N, which enhance mechanical strength and in case of Cr and N also the resistance to pitting corrosion, no significant improvement of electrochemical properties or SCC resistance at all in solutions with high amounts of Cl- ions and temperatures above 100°C was observed.

It could be shown, that the CrMnN21-24-1 does not possess a clear passive range in 3 wt-% $CaCl_2$ solution at 70°C, in contrary to the same environment at ambient temperature. In the case of cyclic polarization, the potential is constantly changing, hence no clear statements on the behaviour of the material under free corrosion potential, if the passive layer is damaged, can be made. Due to this fact, repassivation tests under free corrosion potential were made. It could be shown, that the CrMnN steel does possess a repassivation behaviour, which is just as good as the one of the CrNiMo steels. By single point fatigue experiments it could then be verified, that even under cyclic loading no SCC occurred and fatigue strength is significantly improved compared to the more aggressive environment of 43 wt-% $CaCl_2$ solution and 120°C. By combining cyclic polarization curves and repassivation measurements, sound predictions on the performance of a certain material in a certain environment can be drawn. A wide passive range and good repassivation properties, will result in a good performance under cyclic loading. No pronounced passive range, but good repassivation

behaviour, consequently still results in a good performance under combined attack of mechanical stresses and corrosive environment. If both electrochemical measurements turn out to be unsatisfying, no passive range and no repassivation, performance under mechanical loading, irrespective if constant or cyclic, will not be satisfactory. This empiric model has been proofed by structured experiments with the CrMnN21-24-1 material, as it does not show pronounced passive range in 3 wt-% $CaCl_2$ (Fig. 3b) solution but repassivates (Fig. 4b) under these conditions and single point fatigue experiments. Consequently this empiric model is only applicable if all measurements are performed in one medium at one temperature only. Hence time consuming fatigue experiments can be reduced to an absolute minimum.

Conclusion

- Predictions on SCC and CF behaviour of austenitic stainless steels in chloride environments can be drawn from electrochemical measurements in a certain medium.
- If there is no passive range and no repassivation occurs in one specific medium at one temperature, a material might be unsuitable for applications under combined mechanical and chemical loading.
- In the case of no passive range but good repassivation properties, behaviour under static and cyclic loading will be satisfying.
- If a steel shows a passive range and good repassivation behaviour fatigue strength reduction will be very moderate.

References

[1] J.E. Truman, Effects of nitrogen alloying on corrosion behaviour of high alloy steel, High Nitrogen Steels-HNS88, Lille, France, 18-20 May 1988, p- 229, 1989

[2] R.P. Wei, Electrochemical and microstructural considerations of fatigue crack growth in austenitic stainless steels, Proceedings of the 36th MWSP Conference, ISS-AIM, Vol. 32, p. 541-549, 1995

[3] T. Magnin, Recent advances for corrosion fatigue mechanisms, ISIJ Int. Vol. 35, no. 3, p. 224-225, 231-232. 1995

[4] T. Magnin, Advances in corrosion deformation interactions, Trans Tech Publications Ltd, Switzerland, p.11-15, 69, 80, 87, 88, 1996

[5] E. Kunze, H. Spähn, Korrosion und Korrosionsschutz, Band 1, Wiley-VCH, Weinheim, p. 237-240, 2001

[6] Y.R. Qian, J.R. Cahoon, Crack initiation mechanisms for corrosion fatigue of austenitic stainless steel, Corrosion (USA). Vol. 53, no. 2, p. 135, 1997

[7] T. Magnin, Corrosion – Deformation interactions during environment sensitive damage, Strength of Materials, ICSMA 10, Japan, p. 30, 1994

[8] T. Magnin, D. Delafosse, B. Bayle, C. Bosch, D. Tanguy, Overview of corrosion-deformation interactions during stress corrosion cracking and corrosion fatigue, International Conference on Hydrogen Effects on Materials Behavior and Corrosion Deformation Interactions, USA, p. 567, 569, Sept. 2002

[9] T. Magnin, Corrosion fatigue mechanisms in metallic materials, in P. Marcus (ed.): Corrosion Mechanisms in Theory and Practice, Marcel Dekker Inc., New York – Basel, p. 451-478, 2002

[10] H.S. Kwon, K.A. Yeom, E.A. Cho, Prediction of stress corrosion cracking susceptibility of stainless steels based on repassivation kinetics, Corroion, Vol. 56 (2000), pp 32-40

[11] K.A. Yeom et al., Predicting SCC susceptibility of austenitic stainless steels by rapid scratching electrode technique, Materials Science Forum, Vol. 289-292 (1992), pp 969-978

[12] R.W. Bosch, B. Schepers, M. Vankeerberghen, Development of a scratch test in an autoclave for the measurement of repassivation kinetics of stainless steel in high temperature high pressure water, Electrochimica Acta 49 (2004) 3029-3038

[13] T.A. Adler, R.P. Walters, Repassivation of 304 stainless steel investigated with a single scratch test, Corrosion-NACE 49 (1993) 399-408

[14] T. Yamamoto, et al, Depassivation-repassivation behavior of type-321L stainless steel in NaCl solution investigated by the micro-indentation, Corrosion Science 51 (2009) 1545-1553

[15] S.K. Varma, et al, The effect of electrolyte strength and grain size on the transient current response in Fe-Cr-Ni alloys during a scratch test, Wear 178 (1994) 101-108

[16] P.I. Marshall, G.T. Burstein, The effects of pH on the passivation of 304L stainless steel, Corrosion Science 23 (1983) 1219-1228
[17] G.T. Burstein, G.W. Ashley, Kinetics of repassivation of scratch scars generated on iron in aqueous solutions, Corrosion 40 (1984) 110-115
[18] G.T. Burstein, P.I. Marshall, Growth of passivating films on scratched 304L stainless steel in alkaline solution, Corrosion Science 23 (1983) 125-137
[19] F.M. Song, K.S. Raja, D.A. Jones, A film repassivation kinetic model for potential controlled slower electrode straining, Corrosion Science 48 (2006) 285-307
[20] H. Baba, Y. Katada, Effect of nitrogen on crevice corrosion and repassivation behavior of austenitic stainless steel, Materials Transactions 49 (2008) 579-586
[21] C.J. Park, H.S. Kwon, Comparison of repassivation kinetics of stainless steels in chloride solution, Metals and Materials International 11 (2005) 309-312
[22] G.T. Burstein, P.I. Marshall, The coupled kinetics of film growth and dissolution of stainless steel repassivating in acid solutions, Corrosion Science 24 (1984) 449-462
[23] W.-T. Tsai, A Study of Corrosion Fatigue Crack Growth in Fe-Cr-Ni Alloys, Dissertation Abstracts International Vol. 44 No 1, 1993
[24] F.M. Khoshnaw, A.I. Kheder, F.S.M. Ali, Corrosion behavior of nitrided low alloy steel in chloride solution, Anti-Corrosion Methods and Materials, 54/3, pp 173-179, 2007
[25] M.O. Speidel, Stress Corrosion Cracking and Corrosion Fatigue Fracture Mechanics, Corrosion in Power Generating Equipment; Baden; Switzerland; 19-20 Sept. 1983, pp 85-132, 1984
[26] C.-K. Lin, I.-L. Lan, Fatigue behavior of AISI 347 stainless steel in various environments, Journal of Materials Science 39, pp 6901-6908, 2004
[27] K. Endo, K. Komai, S. Murayma, Influence of Cl- Concentration on Corrosion Fatigue Crack Growth of an Austenitic Stainless Steel, Bulletin of the JSME, Vol. 26, No 218, pp 1281-1287, 1983
[28] I. Aho-Mantila, U. Ehrnsten, R. Kuitunen, A., Kyröläinen, Corrosion Fatigue of three Austenitic Stainless Steels in Sea Water at 20°C and 80°C, Applications of Stainless Steel '92. Vol. 1; Stockholm; Sweden; 9-11 June 1992, pp 458-467, 1992
[29] C.-M. Tseng, H.-Y. Liou, W.-T. Tsai, The influence of nitrogen content on corrosion fatigue crack growth behavior of duplex stainless steel, Materials Science and Engineering A344, pp 190-200, 2003
[30] S.P. Lynch, Progress towards understanding mechanisms of hydrogen embrittlement and stress corrosion cracking, Corrosion 2007, Nashville, NACE, Houston, paper no. 07493, pp. 1-55, 2007
[31] E.I. Meletis, A review of present mechanisms of transgranular stress corrosion cracking, Journal of the Mechanical Behavior of Materials (UK), Vol. 7, no. 1, pp. 1-14, 1996
[32] R. Sonnleitner, Zur Schwingungsrisskorrosion hochfester austenitischer Stähle, Dissertation, Montanuniversität Leoben, 2009
[33] R. Pippan, L. Plöchl, F. Klanner, H. P. Stüwe, The Use of Fatigue Specimens Precracked in Compression for Measuring Threshold Values and Crack Growth, ASTM Journal of Testing and Evaluation (USA), Vol. 22, no.2, pp. 98-103, 1994
[34] R. Pippan, The Growth of Short Cracks Under Cyclic Compression, Fatigue and Fracture of engineering materials and structures, Vol. 9, No. 5, pp. 319-328, 1987
[35] C. Vichytl, R. Sonnleitner, G. Mori, M. Panzenböck, R. Fluch, Crack Growth rate and fracture mechanic investigations of an austenitic stainless steel, Eurocorr 2009, paper no 7900, pp 1-10 (2009)
[36] C. Vichytil, G. Mori, R. Sonnleitner, M. Panzenböck, R. Pippan, R. Fluch, Fracture mechanic investigations of austenitic stainless steels in different cold worked states, Eurocorr 2010, paper no. 9352, pp. 1-11, 2010
[37] C. Vichytil, G. Mori, R. Pippan, M. Panzenböck, R. Fluch, Crack growth rates and corrosion fatigue of austenitic stainless steels in high chloride solutions, Key Engineering Materials, Vols. 488-489 (2012), pp 97-100 (2012)